

Magnetic properties of bulk $\text{Ni}_c\text{Fe}_{1-c}$ alloys, their free surfaces, and related spin-valve systems

P. Weinberger

Center for Computational Materials Science, Technische Universität Wien, Getreidemarkt 9/158, 1060 Vienna, Austria

L. Szunyogh

*Center for Computational Materials Science, Technische Universität Wien, Getreidemarkt 9/158, 1060 Vienna, Austria
and Department of Theoretical Physics, Budapest University of Technology and Economics, Budafoki út. 8, 1111 Budapest, Hungary*

C. Blaas

Center for Computational Materials Science, Technische Universität Wien, Getreidemarkt 9/158, 1060 Vienna, Austria

C. Sommers

Laboratoire de Physique des Solides, Université de Paris-Sud, 91405 Orsay Cedex, France

P. Entel

*Theoretische Physik, Gerhard-Mercator-Universität Duisburg, Lotharstraße 1, D-47048 Duisburg, Germany
and Center for Computational Materials Science, Technische Universität Wien, Getreidemarkt 9/158, 1060 Vienna, Austria*

(Received 5 June 2000; published 12 February 2001)

Using the fully relativistic spin-polarized screened Korringa-Kohn-Rostoker method the magnetic properties of bulk $\text{Ni}_c\text{Fe}_{1-c}$ alloys, their free surfaces, and (free surfaces) of related spin valves of the type $\text{Ni}_c\text{Fe}_{1-c}/\text{Co}_4\text{Cu}_5\text{Co}_4/\text{Ni}_c\text{Fe}_{1-c}$ are calculated. It is found that in the bulk systems the phase transition between fcc and bcc can be described very well in terms of spin and orbital magnetic moments, but also in terms of the magnetic anisotropy energy. The free surfaces and the spin-valve systems differ considerably from the corresponding bulk systems: free surfaces show a reorientation transition from a perpendicular orientation of the magnetization to in-plane at about 60% Ni, whereas the overall in-plane magnetization found in permalloy related spin valves can be mainly related to the contributions of the Co slabs to the band energy part of the magnetic anisotropy energy. In all cases investigated the (spin and orbital) magnetic moments for the free surfaces are considerably enhanced at the surface with similar effects pertaining at the interfaces and the surface of the spin valves.

DOI: 10.1103/PhysRevB.63.094417

PACS number(s): 75.70.Rf, 75.70.Ak, 75.70.Cn

I. INTRODUCTION

Bulk Ni-Fe alloys have intriguing physical properties which involve spinodal ordering in the composition range of permalloys and magnetovolume and martensitic instabilities in the Invar alloys.^{1,2} Renewed interest in Ni-Fe and magnetic Ni-Fe heterostructures is in particular related to recent first-principles calculations showing the extreme softening of the lattice arising from an interaction between magnetic and compositional order/disorder in the alloys,³⁻⁵ an idea that goes back to early work on the influence of concentration fluctuations on magnetism in binary alloys.⁶ In particular, different types of antiferromagnetic^{4,5} and noncollinear³ spin arrangements in the fcc structure lead to additional lattice softening causing the resulting bulk modulus to approach experimental values. Part of the noncollinearity might be related to the long-range oscillatory behavior of the interatomic exchange integral of elemental fcc Fe (see Ref. 7 and references therein) itself which might continue to exist in the predominantly ferromagnetic Ni-Fe alloys. Ni-Fe thin films continue to show the Invar effect. However, the extreme soft magnetic bulk Ni-Fe type seems to disappear as the as-prepared films show high saturation magnetization close to the Slater-Pauling curve.⁸ On the other hand, Ni-Fe alloy layers within Ni-Fe/Cu superlattices with Ni concentrations

lower than the Invar composition show a large thermal expansion and a low magnetic moment which has been associated with superparamagnetic behavior in these alloy layers.⁹

In this short paper we present results of first-principles calculations of bulk Ni-Fe alloys, their free surfaces, and related Ni-Fe/Co/Cu/Co/Ni-Fe spin valves focusing on the change of layer-projected spin and orbital magnetic moments as well as on the change in anisotropy energies with composition over the entire concentration range.

Such combinations of hard and soft magnetic layers are of current interest since they reveal interesting phenomena like exchange-spring magnets (Sm-Co/Fe).¹⁰ Hard/soft magnetic heterostructures allow us to control domain-wall structures and domain-wall magnetoresistance in ferromagnetic films. In addition, the phenomenon of exchange biasing appears in many antiferromagnetic/ferromagnetic bilayer systems. The magnetic anisotropy in these materials is mostly due to the crystal-field interaction of the aspherical $4f$ shells while the transition metals are used to achieve larger magnetic moments and higher transition temperatures. However, these rare-earth/transition-metal heterostructures still suffer from much lower magnetization values than Co or Fe. Therefore it might be of interest to investigate hard/soft magnetic heterostructures involving transition metals and no rare earths.

II. COMPUTATIONAL DETAILS

The fully relativistic spin-polarized screened Korringa-Kohn-Rostoker method¹¹ within the framework of the coherent-potential approximation for layered systems¹² is used to calculate the magnetic properties of bcc and fcc bulk $\text{Ni}_c\text{Fe}_{1-c}$ alloys, their free surfaces, and related spin valves. In order to determine self-consistently within the local-density approximation (LDA) (Ref. 13) the effective potentials and effective exchange fields for each particular system under consideration a minimum of 45 \mathbf{k}_{\parallel} points in the irreducible wedge of the surface Brillouin zone (ISBZ) was used, whereas the band energy part of the magnetic anisotropy energy ΔE_b is based on a much denser \mathbf{k}_{\parallel} grid, namely on a minimum of 990 \mathbf{k}_{\parallel} points per ISBZ. As has been demonstrated several times^{11,15} this ensures an accuracy of the calculated ΔE_b of less than 5% within the theoretical and computational scheme applied.

By using the magnetic force theorem¹⁴ the magnetic anisotropy energy (MAE) consists of two parts,¹¹ namely the difference in the band energy ΔE_b and the magnetic dipole-dipole energy ΔE_{dd} ,

$$E_a = \Delta E_b + \Delta E_{dd}, \quad (1)$$

between two uniform orientations of the magnetization, \mathbf{n} and \mathbf{n}' ,

$$\Delta E_i = E_i(\mathbf{n}) - E_i(\mathbf{n}'), \quad i = b, dd. \quad (2)$$

The band energy part can be split up¹⁵ into layerwise contributions ΔE_b^n ,

$$\Delta E_b = \sum_{n=1}^N \Delta E_b^n, \quad (3)$$

which in turn in the case of (binary) alloyed layers result from the concentration-weighted averaged band energy differences of the individual constituents,¹⁶

$$\Delta E_b^n = \sum_{\alpha=A,B} c_{\alpha}^n \Delta E_b^{n,\alpha}. \quad (4)$$

In general, in Eq. (4) the c_{α}^n refer to layer specific concentrations of atomic species $\alpha=A,B$ and N in Eq. (3) comprises the number of layers of interest. In the present paper the two uniform orientations are chosen as indicated below

$$\begin{aligned} \text{bulk:} \quad & \mathbf{n} = (100) & \mathbf{n}' = (110), \\ \text{free surfaces:} \quad & \mathbf{n} = (110) & \mathbf{n}' = (001), \end{aligned} \quad (5)$$

implying the following classification of preferred orientations:

$$\begin{array}{lll} E_a & \text{bulk} & \text{free surfaces} \\ \leq 0 & \text{along (100)} & \text{in-plane} \\ \geq 0 & \text{along (111)} & \text{perpendicular.} \end{array} \quad (6)$$

It should be noted that for a cubic bulk system with only a fourth-order magnetic anisotropy the easy axis is either (100) or (111), whereas for related semi-infinite systems with

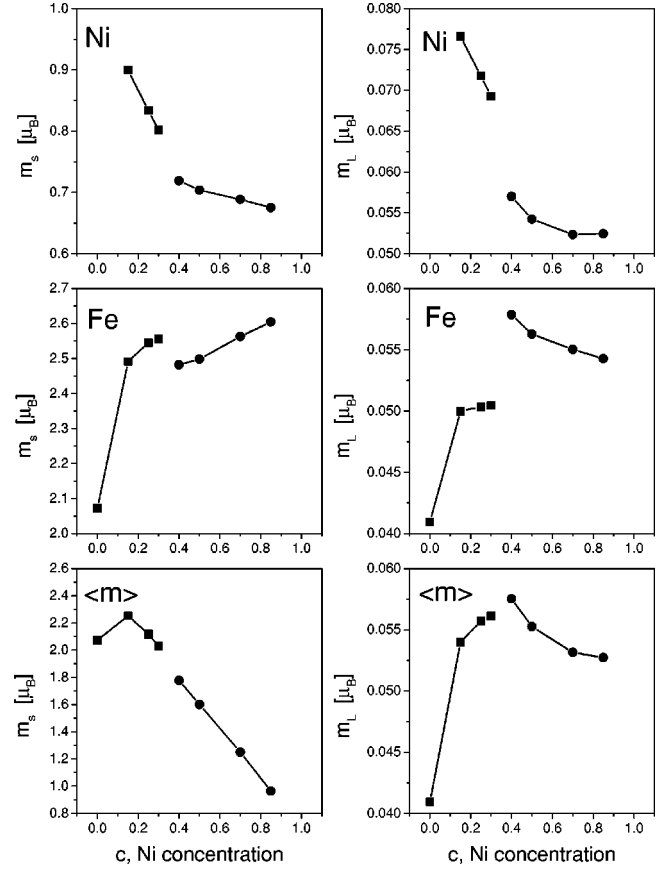


FIG. 1. Variation of the Ni (top), Fe (middle), and the concentration-weighted averaged (bottom) spin (left column) and orbital (right column) magnetic moments in bulk $\text{Ni}_c\text{Fe}_{1-c}$ alloys with respect to the Ni concentration c . Squares and circles refer to a bcc and fcc lattice, respectively.

uniaxial symmetry the rather weak in-plane anisotropy is not taken into account. The layer-resolved concentration-weighted averaged magnetic moments are defined by

$$\langle m^n \rangle = \sum_{\alpha=A,B} c_{\alpha}^n m_{\alpha}^n, \quad (7)$$

an expression that applies for the spin magnetic moments as well as for the orbital magnetic moments. These layer-resolved averaged (total) magnetic moments are also used in turn to calculate the classical magnetic dipole-dipole interaction energy¹⁶ in the case of alloyed layers such as free surfaces of perm-alloy and related spin-valve systems. Note that by neglecting short-range order the magnetic dipole-dipole interaction does not contribute to the MAE of cubic bulk alloys.

III. RESULTS AND DISCUSSION

A. Magnetic moments

In Fig. 1 the spin and orbital moments of the constituents Ni and Fe in the bulk system $\text{Ni}_c\text{Fe}_{1-c}$ are shown together with their respective concentration-weighted averaged moments. In accordance with the well-known experimental

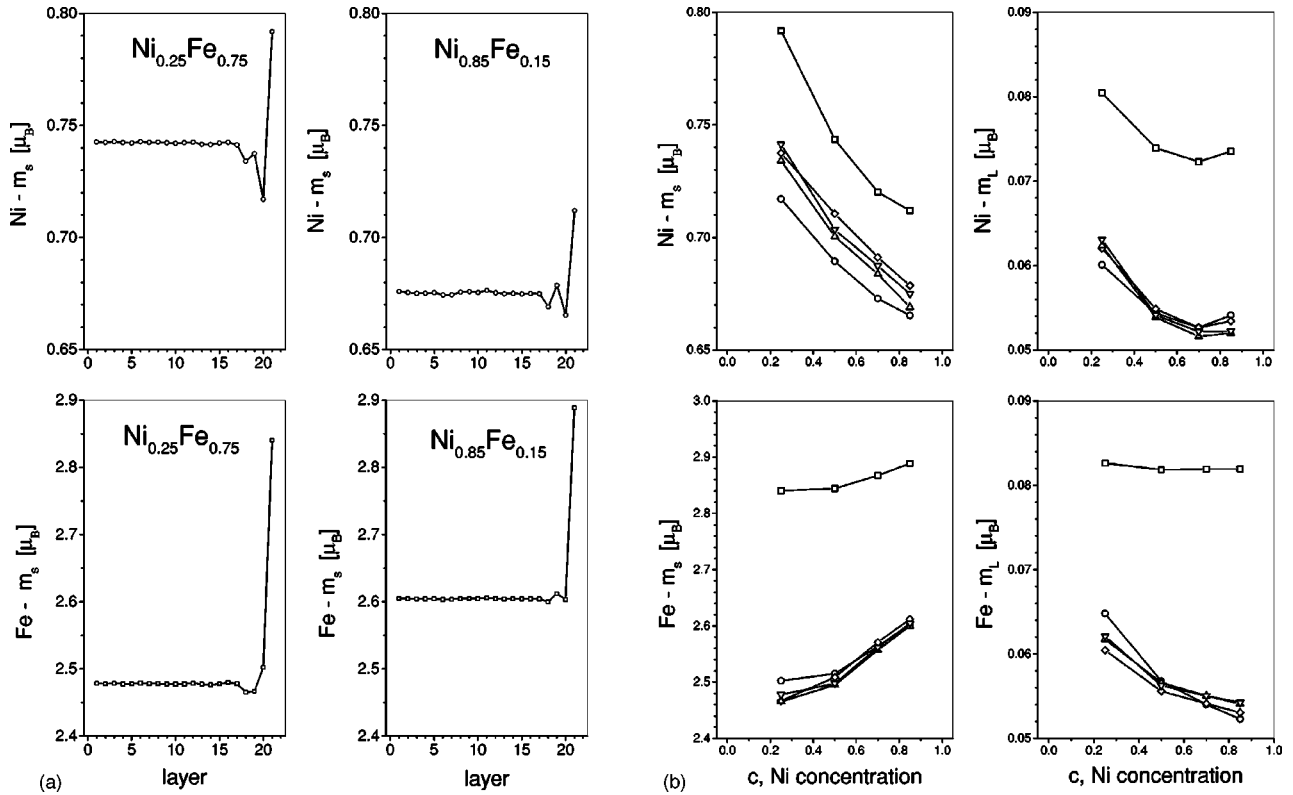


FIG. 2. (a) Variation of the Ni (top) and Fe (bottom) spin magnetic moments in free surfaces of $\text{Ni}_c\text{Fe}_{1-c}$ for $c=0.25$ (left column) and $c=0.85$ (right column) with respect to layers, the topmost (surface) layer being to the right. Note that in this figure for both concentrations a parent fcc lattice applies. (b) Variation of the first five Ni (top) and Fe (bottom) spin (left column) and orbital (right column) magnetic moments in free surfaces of $\text{Ni}_c\text{Fe}_{1-c}$ with respect to the Ni concentration c . The surface layer and the layers below refer in turn to squares, circles, diamonds, up triangles, and down triangles. Note that in this figure for all concentrations a parent fcc lattice applies.

data¹⁷ the phase transition between bcc- and fcc-like phases occurs at about 35% Ni. In order to show on the Fe-rich side the drastic increase of both the spin and the orbital moment with increasing Ni concentration in the case of the Fe constituent also the corresponding values for pure bcc bulk Fe are included. As can be seen the Ni-like as well as the Fe-like moments exhibit completely different behavior in the bcc- and fcc-like phases, the jump in the Fe orbital moment at the phase boundary being almost spectacular. In terms of the concentration-weighted averaged moments the phase transition appears to cause less dramatic effects: a different slope for the averaged spin moment and a kind of peak for the orbital moment when going from the bcc to the fcc phase.

As is to be expected in free surfaces of $\text{Ni}_c\text{Fe}_{1-c}$ the most significant differences with respect to the bulk occur in the surface region. In Fig. 2(a) the layer-resolved Ni-like and Fe-like spin moments are followed from the surface (right) to the very interior of two selected systems, characteristic for the whole series of alloys. As can be seen, bulklike features set in about six to seven layers below the surface, the moments in the surface layer being substantially increased as compared to the respective bulk system. For the fcc phase the concentration dependence of the spin and orbital magnetic moments in the first five layers, shown in Fig. 2(b), resembles the corresponding trends in the bulk (see also Fig. 1). Again the prominent role of the surface layer is obvious.

It should be noted that because of the oscillations clearly to be seen in Fig. 2(a), the curves in Fig. 2(b), read from top to bottom, do not correspond to a sequential viewing of layers from the surface to the interior of these semi-infinite systems.

Typical $\text{Ni}_c\text{Fe}_{1-c}$ related spin valves consist of a rather thick layer of permalloy (Py) followed by four to six layers of Co separated from another four to six Co layers by five to seven layers of Cu. The whole system is then coated with a rather thin layer of permalloy. In here such a system is modeled by $\text{Ni}_c\text{Fe}_{1-c}(001)/(\text{Ni}_c\text{Fe}_{1-c})_{12}/\text{Co}_4\text{Cu}_5\text{Co}_4/(\text{Ni}_c\text{Fe}_{1-c})_3/\text{Vac}$, where Vac indicates the free surface side and a sufficient number (12) of $\text{Ni}_c\text{Fe}_{1-c}$ layers guarantees a smooth, self-consistent matching to the $\text{Ni}_c\text{Fe}_{1-c}$ substrate. It should be noted that this system reflects very realistically the actual giant magnetoresistance (GMR) devices based on permalloy.¹⁸

The top of Fig. 3 shows the layer-resolved spin magnetic moments in this spin-valve system for two different concentrations of Ni. In particular the case of $c=0.85$ is relevant for practical purposes as from this part of Fig. 3 the technological phrase of “using permalloy as a soft magnetic material” can directly be read off. For both concentrations the changes in the layer-resolved magnetic moments at the Py/Co interfaces and at the surface are immediately evident. The left bottom entry of Fig. 3 shows the Co moment in comparison

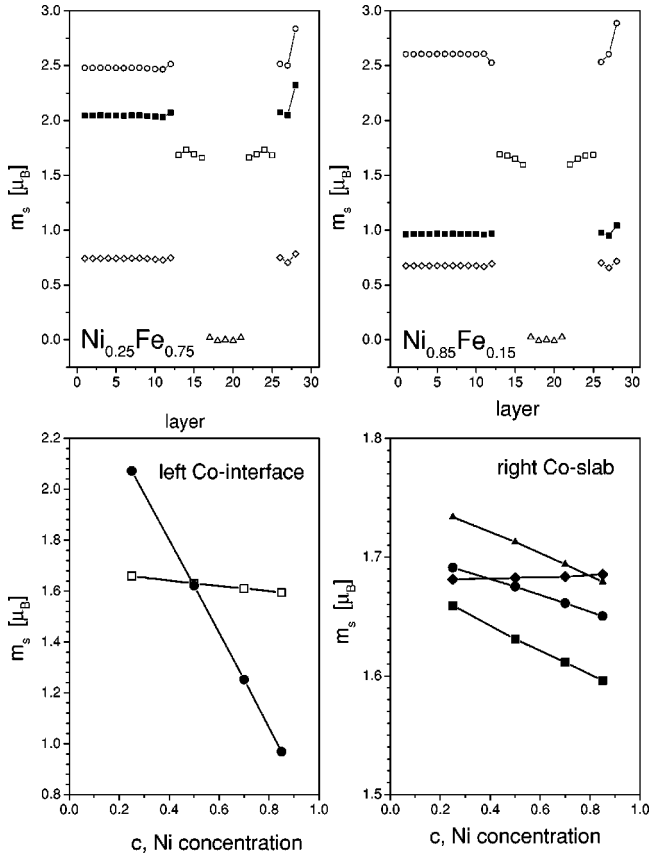


FIG. 3. Top: Variation of the spin magnetic moments with respect to layers in the spin-valve system $\text{Ni}_c\text{Fe}_{1-c}/(\text{Ni}_c\text{Fe}_{1-c})_{12}/\text{Co}_4\text{Cu}_5\text{Co}_4/(\text{Ni}_c\text{Fe}_{1-c})_3/\text{Vac}$ for $c=0.25$ (left) and $c=0.85$ (right). The Fe, Ni, and concentration-weighted averaged moments refer to open circles, open diamonds, and full squares, respectively, the Co moments to open squares, the nearly vanishing induced Cu moments are indicated by open triangles. Bottom left: Variation of the concentration-weighted averaged spin magnetic moment (full circles) and of the Co spin magnetic moment (empty squares) corresponding to the two layers forming the left $\text{Ni}_c\text{Fe}_{1-c}/\text{Co}$ interface with respect to the Ni concentration c . Bottom right: Variation of the Co spin magnetic moments in the four layers forming the right Co slab with respect to the Ni concentration c . The Co layer next to the permalloy is shown with diamonds, the next ones with triangles, circles, and squares for the Co layer next to the Cu. Note that in all cases shown in this figure a fcc parent lattice applies.

to the concentration-weighted averaged moment of that Py layer forming the left interface as a function of the Ni concentration. As is to be expected by varying the Ni concentration one actually can tune the averaged moment to the size of the Co moment: at about 50% Ni the Py layers look magnetically like Co layers. Quite interesting is the variation of the Co moments in the right Co slab, since the moment in the Co layer forming the right Co/Py interface is least affected by changing the Ni concentration while the variations of the moment in the Co layer interfacing with the Cu spacer are biggest. It also should be noted that the layerwise distribution of moments in the left and right Co slab is not symmetric, reflecting thus the different magnetic behavior of the thin Py slab (on the right) forming the surface near region as

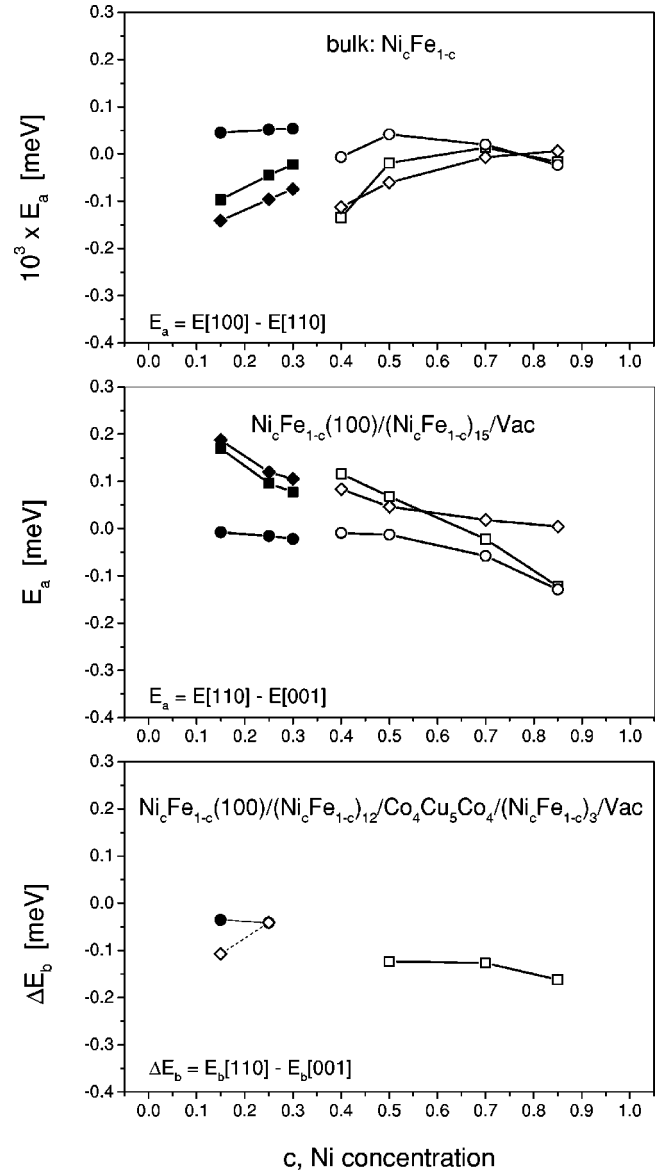


FIG. 4. Magnetic anisotropy energy (squares) in $\text{Ni}_c\text{Fe}_{1-c}$ related systems with respect to the Ni concentration c . Top: bulk (MAE/atom); middle: free surfaces (MAE/unit of area); bottom: $\text{Ni}_c\text{Fe}_{1-c}$ related spin valves (MAE/unit of area). Full symbols refer to bcc, open symbols to fcc related systems. In the bulk and free surface cases also the concentration-weighted contributions of Ni (circles) and Fe (diamonds) to the total magnetic anisotropy energy are shown. In the case of the spin valves only the band energy contribution to the magnetic anisotropy energy is shown (this time, diamonds refer to a fictitious fcc lattice).

compared to its thick counterpart (on the left) matching up to the substrate. Quite clearly at or very close to the surface the corresponding Py slab shows the same features as free surfaces of Py, namely a substantial increase of the component-resolved as well as of the averaged spin moments.

B. Magnetic anisotropy energy

In Fig. 4 the magnetic anisotropy energy for the bulk systems, free surfaces of $\text{Ni}_c\text{Fe}_{1-c}$, and in Py-related spin

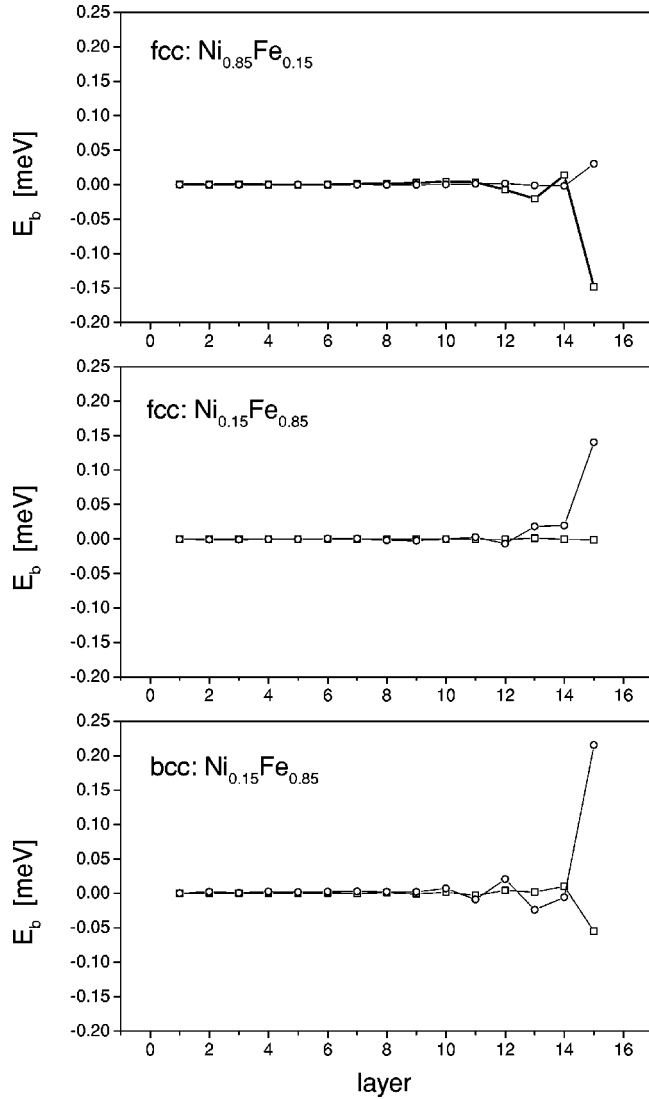


FIG. 5. Layer- and component-resolved contributions to the band energy part of the anisotropy energy in free surfaces of $\text{Ni}_c\text{Fe}_{1-c}$. Top: fcc $\text{Ni}_{0.85}\text{Fe}_{0.15}$; middle: fcc $\text{Ni}_{0.15}\text{Fe}_{0.85}$; bottom: bcc $\text{Ni}_{0.15}\text{Fe}_{0.85}$. The concentration-weighted Ni and Fe contributions are shown as open squares and circles, respectively.

valves is displayed. Although their shapes and orders of magnitude are completely different, at the phase boundary between bcc and fcc significant changes in the magnetic anisotropy energy occur for free surfaces as well as in the bulk. As will be discussed in detail in the context of Fig. 6, in the spin-valve systems the structural differences seem to be of little importance: for $c = 0.25$ virtually the same ΔE_b applies for a bcc and a fcc parent lattice.¹⁹ Furthermore, in the spin valves the preferred orientation is always in-plane as can be seen immediately from the negative band energy contribution. The negative magnetic dipole-dipole energy contribution (not taken into account in this particular case), see also Eq. (1), only enhances this tendency.

Inspecting now the curves for the bulk systems and the free surfaces most prominently the difference in scale has to be noted: the bulk anisotropy energy is by a factor 10^3 smaller than the corresponding free surface case. In the bulk

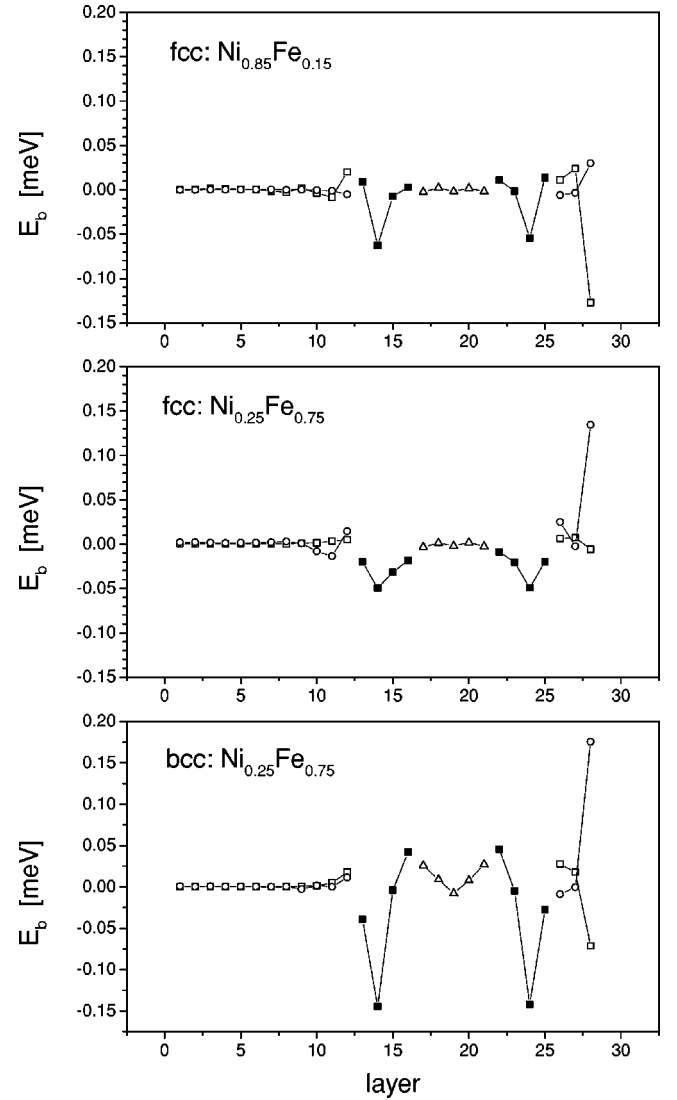


FIG. 6. Layer- and component-resolved contributions to the band energy part of the anisotropy energy in $\text{Ni}_c\text{Fe}_{1-c}$ related spin valves. Top: fcc $\text{Ni}_{0.85}\text{Fe}_{0.15}$; middle: fcc $\text{Ni}_{0.25}\text{Fe}_{0.75}$; bottom: bcc $\text{Ni}_{0.25}\text{Fe}_{0.75}$. The concentration-weighted Ni and Fe contributions are shown as open squares and circles, the Co and Cu contributions from the “active part” of the spin valve, namely $\text{Co}_4\text{Cu}_5\text{Co}_4$, as full squares and open triangles, respectively.

systems around 70% Ni the anisotropy energy nearly vanishes. For all Ni concentrations lower than 0.85, the Fe-like contribution seems to be the driving force for selecting the (100) direction as easy axis. This implies that the same easy axis pertains for bcc- and fcc-like $\text{Ni}_c\text{Fe}_{1-c}$ bulk systems.

Around 60% Ni the free surfaces show a reorientation transition from perpendicular to in plane, for higher concentrations of Ni the preferred orientation of the magnetization is in plane. It is remarkable that independent of the structure, below 60% Ni a perpendicular orientation is more favorable. As can be seen the reorientation transition for free surfaces of $\text{Ni}_c\text{Fe}_{1-c}$ is mainly caused by the Ni contribution. As the bulk easy axis lies in plane, the perpendicular surface anisotropy in the case of (001) surfaces can give rise to a particularly interesting phenomenon, namely, noncollinear magnetic

configurations can occur: the orientation of the magnetization rotates from in plane to perpendicular when going from bulklike layers to the surface.²⁰ Although the study of such configurations is out of the scope of the present paper, it is important to note that they indeed can influence the magnetotransport in such systems.

In Fig. 5 the layer-resolved contributions to the band energy part of the anisotropy energy are shown in terms of concentration-weighted componentlike contributions. As can be seen from this figure the first five to six layers forming the surface region are different from those in the interior of the systems, whereby the surface layer gives the biggest contribution. From this figure it is also evident that it is essentially the large negative Ni contribution in the surface layer that drives the reorientation transition, since the Fe contributions are positive, i.e., favor a perpendicular orientation of the magnetization. From the two lower parts of Fig. 5 follows that the oscillations into the interior of these systems are considerably stronger in the case of a bcc parent lattice than for a fcc parent lattice.

In Fig. 6 finally the layer- (and component-) resolved band energy contributions to the magnetic anisotropy energy are displayed for permalloy related spin valves. For these kinds of systems two different major effects have to be considered, namely the contributions from the so-called “active part” of the spin valve, the $\text{Co}_4\text{Cu}_5\text{Co}_4$ unit, and from the surface region. In all cases the sum over the Co-like contributions is negative, while in the surface region a similar behavior as discussed above for free surfaces applies. As already mentioned in the spin-valve systems the preferred orientation is always in-plane. For Ni-rich permalloy spin valves this is caused by the Ni-like contribution in the surface region and by the Co-layer overnext to the corresponding Py/Co interface. Just like in the case of free surfaces as the Fe concentration increases also the positive Fe contribution from the surface layer increases, which, however, is out-weighted by the contributions from the Co slabs such that the preferred orientation of the magnetization remains in plane. Because of a very delicate balance between surface Fe and Co-slab contributions in the very special case of $\text{Ni}_{0.25}\text{Fe}_{0.75}$ the bcc related spin valve has virtually the same ΔE_b as in a (fictitious) fcc spin valve.

Surface (interface) roughness and intermixing effects presumably play an important role in spin-valve systems. Studies in terms of the coherent-potential approximation revealed that interdiffusion at the interfaces of magnetic and nonmagnetic materials usually wipes out magnetic anisotropy effects.²² In the spin valves studied in here relevant intermixing can be expected predominantly at the Co/Cu interfaces, which, as can be seen from Fig. 6, contribute only very little

to the MAE. Therefore we do not expect significant changes in the MAE due to intermixing effects at the Co/Cu interfaces. On the contrary, intermixing at these interfaces is of crucial importance for magnetotransport as was demonstrated in a case study by Blaas *et al.*²³

IV. CONCLUSION

It was the aim of this paper to show that even well-known, well-used materials like permalloy have undiscovered and surprising properties. In particular, when choosing these materials for new kinds of devices by making use of their surface properties or by forming interfaces with other metals like in spin valves, it seems to be almost fatal to simply take into account only some of their bulk properties. Clearly enough systems like $\text{Ni}_c\text{Fe}_{1-c}$ “suffered” from their applications as reliable bulk permanent magnets. However, considering that this particular system shows a surface driven reorientation transition, whose temperature dependence near the critical concentration might be of quite some technological importance, and considering that in (commercial) GMR devices based on permalloy the electronic structure and the magnetic properties are completely different from those in the bulk, it appears to be necessary to review this class of materials from a different point of view, namely in terms of surface and interface magnetism. It will be shown in a forthcoming paper²¹ that the results obtained here put into a proper theory of electrical transport not only describe the bulklike (normal) resistivities for $\text{Ni}_c\text{Fe}_{1-c}$ extremely well, but also the current-in-plane (CIP) GMR ratio in related spin valves. The fact that the averaged moment in this system can be tuned by the Ni concentration might very well trigger other applications based on surface or interface magnetic properties, or, oppositely expressed, create the demand to investigate also surface related magnetic properties of different permalloy systems.

ACKNOWLEDGMENTS

This paper resulted from a collaboration partially funded by the TMR network (Contract No. EMRX-CT96-0089) and by the Research and Technological Cooperation between Austria and Hungary (OMFB-BMAA, Contract No. A-35/98). Financial support was provided also by the Center for Computational Materials Science (Contract No. GZ 45.442), the Austrian Science Foundation (Contract Nos. P12146 and T27-TPH), and the Hungarian National Science Foundation (Contract Nos. OTKA T030240 and T029813). We also wish to thank the computing center IDRIS at Orsay as part of the calculations were performed on their Cray T3E machine.

¹E. F. Wassermann, in *Ferromagnetic Materials*, edited by K. H. J. Buschow and E. P. Wohlfarth (Noth-Holland, Amsterdam, 1990), p. 240.

²E. F. Wassermann, M. Acet, P. Entel, and W. Pepperhoff, *J. Magn. Soc. Jpn.* **23**, 385 (1999).

³M. van Schilfgaarde, I. A. Abrikosov, and B. Johansson, *Nature (London)* **400**, 46 (1999).

⁴P. James, O. Eriksson, B. Johansson, and I. A. Abrikosov, *Phys. Rev. B* **59**, 419 (1999).

⁵P. Entel, E. Hoffmann, H. C. Herper, E. F. Wassermann, V.

- Crison, H. Ebert, and H. Akai, *J. Magn. Soc. Jpn.* (to be published).
- ⁶J. B. Staunton, D. D. Johnson, and B. L. Gyorffy, *J. Appl. Phys.* **61**, 3693 (1987).
- ⁷Y.-M. Zhou, D.-S. Wang, and Y. Kawazoe, *Phys. Rev. B* **59**, 8387 (1999).
- ⁸G. Dumpich, J. Kästner, U. Kirschbaum, H. Mühlbauer, J. Liang, Th. Lübeck, and E. F. Wassermann, *Phys. Rev. B* **46**, 9258 (1992).
- ⁹W. Tang, Ch. Gerhards, J. Heise, and H. Zabel, *J. Magn. Mater.* **191**, 45 (1999).
- ¹⁰E. E. Fullerton, J. S. Jiang, and S. D. Bader, *J. Magn. Mater.* **200**, 392 (1999).
- ¹¹L. Szunyogh, B. Újfalussy, and P. Weinberger, *Phys. Rev. B* **51**, 9552 (1995).
- ¹²P. Weinberger, P. M. Levy, J. Banhart, L. Szunyogh, and B. Újfalussy, *J. Phys.: Condens. Matter* **8**, 7677 (1996).
- ¹³S. H. Vosko, L. Wilk, and M. Nusair, *Can. J. Phys.* **58**, 1200 (1980).
- ¹⁴H. J. F. Jansen, *Phys. Rev. B* **59**, 4699 (1999).
- ¹⁵B. Újfalussy, L. Szunyogh, and P. Weinberger, *Phys. Rev. B* **54**, 9883 (1996); **55**, 14 392 (1997); L. Szunyogh, B. Újfalussy, C. Blaas, U. Pustogowa, C. Sommers, and P. Weinberger, *ibid.* **56**, 14 036 (1997); J. Zabloudil, C. Uiberacker, U. Pustogowa, C. Blaas, L. Szunyogh, C. Sommers, and P. Weinberger, *ibid.* **57**, 7804 (1998); C. Uiberacker, J. Zabloudil, P. Weinberger, L. Szunyogh, and C. Sommers, *Phys. Rev. Lett.* **82**, 1289 (1999); for a review, see P. Weinberger and L. Szunyogh, *Comput. Mater. Sci.* **17**, 414 (2000).
- ¹⁶J. Zabloudil, L. Szunyogh, U. Pustogowa, and P. Weinberger, *Phys. Rev. B* **58**, 6316 (1998).
- ¹⁷K. Schroeder, *CRC Handbook of Electrical Resistivities of Binary Metallic Alloys* (CRC Press Inc., Boca Raton, FL, 1983), p. 247.
- ¹⁸E. Chen and S. Tehrani, *GMR Film for PSV MRAM Cell*, U. S. Patent 5,702,831, Issued Dec. 30, 1997.
- ¹⁹For a discussion of the concept of parent lattices, see, e.g., P. Weinberger, *Philos. Mag. B* **75**, 509 (1997).
- ²⁰L. Udvardi, R. Király, L. Szunyogh, F. Denat, M. B. Taylor, B. L. Györffy, B. Újfalussy, and C. Uiberacker, *J. Magn. Mater.* **183**, 283 (1998).
- ²¹C. Blaas, P. Weinberger, L. Szunyogh, P. M. Levy, and C. Sommers (unpublished).
- ²²L. Szunyogh, P. Weinberger, and C. Sommers, *Phys. Rev. B* **60**, 11 910 (1999).
- ²³C. Blaas, P. Weinberger, L. Szunyogh, P. M. Levy, and C. Sommers, *Phys. Rev. B* **60**, 492 (1999).